Interdigitated capacitance sensors in the mm scale with sub-femtoFarad resolution suitable for monitoring processes in liquid films

A. Guadarrama-Santana[a,*], A. García-Valenzuela[a], F. Pérez-Jiménez[a] and L. Polo-Parada[b]
[a]*Centro de Ciencias Aplicadas y Desarrollo Tecnológico, Universidad Nacional Autónoma de México, Apartado Postal 70-186, Distrito Federal 04510, México,*
[*]*Phone: +52-55-56228602 ext. 1116*
e-mail: asur.guadarrama@ccadet.unam.mx
[b]*University of Missouri Department of Medical Pharmacology and Physiology, Medical School, Dalton Cardiovascular Research Center 134 Research Park Drive Rd. Columbia, MO 65211 USA,*
e-mail: poloparadal@missouri.edu

Received 28 April 2014; accepted 19 September 2014

We propose and analyze a high resolution capacitive sensor appropriate for monitoring physical or chemical processes in liquid films. The proposed sensor is based on a planar interdigitated capacitor with planar electrodes of dimensions in the milimeter scale. The electric field between electrodes extend above the plane of the electrodes up to a few milimeters and thus permits placing a dielectric container with a liquid film on top and still be sensitive to changes in the liquid film. First, we present numerical calculations of the capacitance of an interdigitated sensor as a function of the thickness and dielectric constant of a film placed on top of it using a finite element method. Then, we describe a suitable electronic system to sense with very high-resolution capacitance variations of the sensor by measuring the phase lag and amplitude change of a sinusoidal current signal passing through it. This is accomplished by subtracting a stable sinusoidal current of the same frequency going through a reference device. Initially the system is balanced by adjusting the reference current to cancel out the net output current. In this way, we compensate parasitic capacitances due to electronics, wiring and system hardware as well. When the capacitance of the sensor element varies the system gets unbalanced and a net current appears. The resulting current is measured with a locking-amplifier. To illustrate the sensitivity and resolution achieved by the sensing system, we present results of monitoring the capacitance of the sensor during the evaporation of liquid solvent films and discuss the time-evolution of the registered signals. The floor noise throughout the measurements was in the order of 50 atto-Farads while the signal varied in the range of several femto-Farads.

Keywords: Capacitance; interdigitated; electrodes; dielectric; solvent; evaporation.

PACS: 84.37.+q; 77.22.-d; 64.70.F-; 07.07.Df

1. Introduction

Interdigitated Capacitance Sensors (IDCS) have been used in different fields of industry as well as in physical, chemical, biochemical and medical research [1]. They offer practical advantages for material characterization by means of electrical capacitance measurements due to frequency dependent dielectric properties of polymeric layers, liquids, micro-granular and macro-granular matter.

Often, the time evolution of a physical property in a Material Under Test (MUT) can be obtained by means of a dielectric constant measuring-system [2]. In general, both the relative permittivity (which can be complex at high frequencies) and conductivity of a material contribute to the dielectric constant of a material. In an IDCS the sensitivity to variations of the conductivity or permittivity depends on the penetration of the electric field inside a MUT contributing to the capacitance and impedance between electrodes [3]. Depending on the geometric configuration of the electrodes the electric field lines can penetrate deeper or less deep. The capacitance of an IDCS always depends on the dielectric properties of the MUT and the geometry of the electrodes. The electrode pattern needs to be repeated several times in order to strengthen the measured signal. In these cases, the measured fringing field capacitance is usually considerably low. IDCS have widespread applications. Biochemical sensors for DNA detection [4-6] and capacitive chemical sensors [7-10] constitute a major portion of all IDC sensors.

An important advantage of planar sensors is that only one of the surfaces of the Material Under Test (MUT) is directly in contact with the electrodes, leaving the other surface of the MUT interacting with the environment and allowing the IDCS to sense physical or chemical variables of the environment. For instance, for a chemical sensor a chemically sensitive layer is deposited on top of IDC electrodes in order to sense the absorption of a gas, concentration of a particular chemical in the environment, moisture, heat exchange with the surrounding medium, organic impurities or electric biosignals in the case of biological samples [11].

When the sensitive layer (commonly a polymer) interacts with the chemicals present in the environment, the chemically sensitive layer changes its conductivity (σ), dielectric constant (ε) or its effective thickness (d). The interdigitated capacitance (IDC) chemical sensor can then detect a change in capacitance and/or impedance due to a change of the dielectric constant and thickness of the layer. IDC chemical sensors have been investigated by many researchers because they are

inexpensive to manufacture and easily integrated with other sensing components and signal processing electronics [3].

There are other applications in which IDCS are useful, such as microfluidic devices [2], Surface Acoustic Wave devices for consumer electronics and telecommunication applications [12] and microwave integrated circuits [13-15]. Also, IDCS are suitable devices for Non-Destructive Testing (NDT) [16]. As already mentioned, a physical parameter of interest of the MUT can be obtained indirectly by means of the relation with the effective dielectric function. Thus, these devices can also be used advantageously to sense temporal changes of physical or chemical variables of a MUT [17].

Recently, polymer nanoparticles have been applied in a wide range of fields as electronics, photonics, conducting materials, sensors, medicine, biotechnology, pollution control and environmental technology. Physico-chemicals factors as solvent composition, evaporation velocity, humidity, temperature, etc., are involved in the solvent evaporation process which is a very important method for the preparation technique of polymer nanoparticles, thin structured micro and nanoparticles coatings, [18,19].

Our aim is to study the sensitivity of IDCS theoretically and propose and implement a high-resolution electronic system to measure capacitance variations of the IDCS. Also in this work, we are interested in understanding the sensitivity and resolutions achievable with IDCS for monitoring the evaporation process of liquid films.

In Sec. 2 we present an analysis of the sensitivity of IDCSs to dielectric layers by means of Finite Element Method simulations. 3D simulations are presented in order to obtain its response curves of capacitance C as a function of the dielectric constant k and thickness d of the dielectric layer. It is not difficult to understand that for layers thicker than some minimum value $d_{\min}$ the capacitance depends only on the dielectric constant of the layer and not on its thickness. The simulations allow us to estimate the value of $d_{\min}$ for the example that was simulated, as well as the maximum sensitivity of the interdigitated sensor. Also, the dynamic range of the sensor and the maximum capacitance value are obtained from the simulated curves in order to characterize the response of the sensor. Then in Sec. 3 we propose and describe an experimental setup of a low noise Temporal Capacitive Measuring System (TCMS) for characterizing physico-chemical processes by sensing temporal capacitance changes with interdigitated sensors. The signal of the TCMS is conditioned electronically before it gets into a Lock-in Amplifier which extracts the contribution of the MUT from the surrounding noise, with a reference signal of 10 KHz central frequency. The capacitance values during a physico-chemical process are proportional to the imaginary part of the current signal passing through the MUT. In order to illustrate the sensitivity and resolution of the system in Sec. 4 we present examples of monitoring the evaporation of a solvent film on top of the IDCS. An attempt to explain the capacitance signal over time during the experiments is also presented. Finally, in Sec. 5 we provide our conclusions along with some discussion.

2. Numerical simulations with the Finite Element Method

Interdigitated capacitors consist of conductive coplanar electrodes or fingers placed parallel to each other with a gap g between them. They are deposited on a plane surface of a dielectric substrate. The surface where the electrodes are deposited is called the sensitive surface [11]. The finger electrodes connected to the source voltage are called the driving electrodes whereas those connected to ground are referred to as the sensing electrodes.

In order to gain some insight into the performance of IDCS to sense a dielectric layer on top of it we performed 3D simulations using a Finite Element Method (FEM) of an interdigitated capacitor with and without a dielectric layer on top of it. We calculated the capacitance for different values of the dielectric constant and thickness of the dielectric layer (that is, the MUT).

The geometry of the simulated IDCS is shown in Figs. 1(a) and 1(b). We considered a six finger interdigitated sensor deposited on the surface of a homogeneous substrate of dielectric constant $k_s = 4.8$ variable with thickness h_s, and surface area of 1.6×1.5 cm^2. The fingers electrodes were assumed to have a thickness of $h_e = 25$ μm, a width $w = 1$ mm, and length $l = 9$ mm. The gap between electrodes was assumed to be $g = 1$ mm. The MUT surface area was 1.4 cm^2 with thickness d and dielectric constant k, both variables.

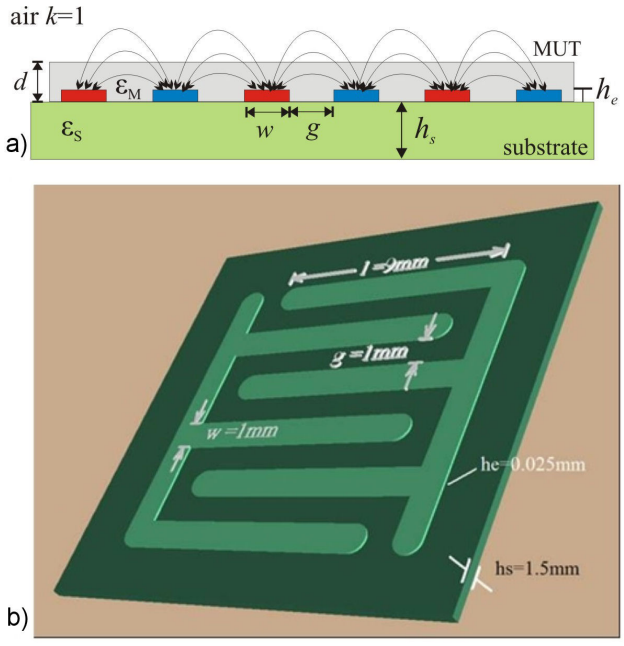

FIGURE 1. a) Cross section of six finger interdigitated capacitor sensor with fringing electric fields and constant parameters used for 3D Finite Element Method simulations. b) Complete six finger interdigitated capacitor sensor used for 3D Finite Element Method simulations.

The simulations were carried out in the electrostatic approximation with a potential difference of $V = 1$ volt between driving and sensing electrodes. We calculated the net charge on the driving electrodes, Q, and obtained the capacitance simply as,

$$C = \frac{Q}{V} \tag{1}$$

The capacitance C was calculated for different values of the dielectric constant k and thickness d of the MUT to obtain the performance parameters of the IDCS [20,21].

The charge on the driving electrodes was calculated with the following integrals over the entire surface of the driving electrodes, including the electrode connecting the fingers (see Fig. 1b),

$$Q = \varepsilon_S \int_{\Sigma_S} E \cdot \hat{n} ds + \varepsilon_M \int_{\Sigma_M} E \cdot \hat{n} ds, \tag{2}$$

where Σ_S is the surface of the electrodes in contact with substrate of electric permittivity ε_S and Σ_M is the fraction of the electrode's surface in contact with the upper medium (the MUT) of electric permittivity $\varepsilon_M = k\varepsilon_0$.

Graphs of C vs k and C vs d were obtained from the FEM simulations for thickness values from $d = 100$ μm to $d = 2$ mm and dielectric constant values from $k = 2$ to $k = 20$. These are shown in Fig. 2 and 3 respectively. The black star mark represents the capacitance value C for the interdigitated capacitor without MUT.

In Fig. 2 we can appreciate a linear variation of the capacitance C with the dielectric constant k for different thicknesses d of the MUT film. The minimum capacitance value, corresponding to $k = 1$, that is when there is no MUT over the interdigitated capacitor. When the dielectric constant k is

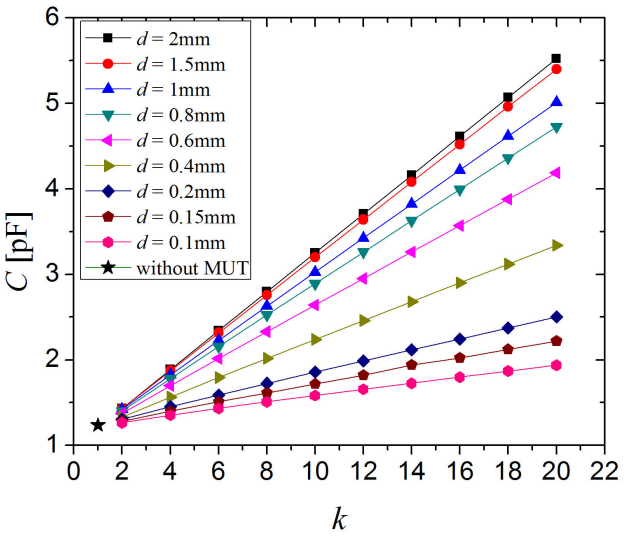

FIGURE 2. C vs k curves with different thicknesses d of the MUT. The black star mark represents the capacitance value C without a MUT, that is, for $k = 1$.

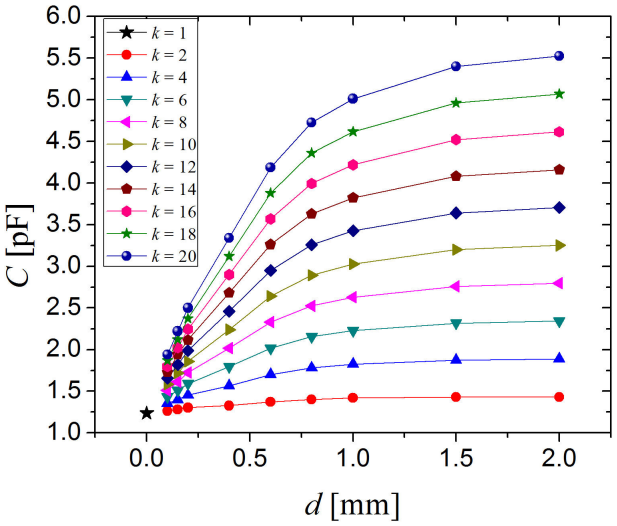

FIGURE 3. C vs d curves with different dielectric constant k of the MUT. The black star mark represents the capacitance value C without a MUT, that is, for $k = 1$.

increased the capacitance value is also increased for any thickness d. However, for a MUT film of thickness between 1.5 mm and 2 mm and for larger values, the capacitance variation versus k is nearly the same. Thus, the C vs k curves show that the capacitance of the MUT tends to be independent of d for $d \geq 2$ mm in this specific geometry. Furthermore, the sensitivity $S_{\max}$ for a thickness larger than $d_{\min} = 2$ mm can be determined from the slope of the C vs k curves, that is

$$S_{k,\max} = \left.\frac{\partial C}{\partial k}\right|_{d_{\min}}. \tag{3}$$

The expression (3) represents the ratio of changes in capacitance C to changes in dielectric constant k of the MUT for a thickness $d_{\min}$ and larger. For instance, with $d_{\min} = 2$ mm and for $k_1 = 6$, $k_2 = 8$ we obtain their respective capacitance values $C_1 = 2.343$ pF and $C_2 = 2.797$ pF, from curves of Fig. 1. With this data, the sensitivity $S_{k,\max}$ for $d_{\min}$ can be calculated form the slope $S_{k,\max} \approx 0.23$ pF.

From Fig. 3 we see that the sensitivity to thickness variations of the MUT, $S_d = \partial C/\partial d$, depends on its thickness and dielectric constant. It is larger for smaller thicknesses. In fact it is relatively constant for any value of k for thicknesses d smaller than about 0.5 mm. For larger thicknesses the sensitivity decays approaching zero at a thickness of $d_{\min} = 2$ mm. The sensitivity to thickness variations is about $S_d \approx 4$ pF/mm for a dielectric constant of $k = 20$ and a thickness less than 0.5 mm. This value decreases about ten fold for a dielectric constant of $k = 4$.

In the case analyzed numerically here we see that the thickness $d_{\min}$ is twice the gap g between electrodes,

$$d_{\min} \cong 2g. \tag{4}$$

The values just stated give us an idea of the sensitivity of an interdigitated sensor to a dielectric layer on top of it. Of

course these values will change for different geometries, that is, for different values of g and w and for larger number of fingers. Nevertheless, if the geometrical aspects of the IDCS are kept constant the values just given can be easily translated to other scales in view of what we call the isotropic scaling law of the electrical capacitance [22]. For instance, as long as $w = g$ in the device, $l = 9w$ and he is much smaller than other dimensions Eq. (4) will be true at any scale for a six finger IDCS.

The value of $d_{\min}$ also tells us how deep the electric field lines penetrate into the MUT [3]. In many applications it is necessary to isolate the electrodes with a dielectric coating. It is convenient that its thickness d be as thin as possible compared to $d_{\min}$ in order to use the maximum dynamic range of the capacitive sensor for a sample of interest placed above the sensitive surface of the sensor.

3. Temporal Capacitive Measuring System (TCMS)

The methods commonly used to measure electrical capacitance and interrogate interdigitated sensors are based on Voltage Sensing Circuits, Current Sensing Circuits and Phase Detection Circuits [17,21]. In all sensing methods an AC driving voltage is required to generate an electric field that penetrates the MUT and the dielectric substrate as well. Perturbations of the electric field by the MUT change the capacitance between the interdigitated electrodes. In general it is possible to monitor physical or chemical changes in the MUT from measuring the capacitance variations on time. The time scale in which one can monitor changes in the MUT will depend on the frequency used to measure the capacitance of the IDCS. If one is using a frequency f to measure the capacitance the IDCS will be limited to sense changes of the MUT over times much larger than $1/f$.

As in most capacitance sensors, it will be necessary to compensate for stray capacitances in the measuring system in order to extract the contribution to the capacitance of the MUT placed on the sensitive surface of the IDCS [23].

The capacitance variations due to changes in a thin dielectric film on top of a IDCS will in general be very small compared to the capacitance of the IDCS by itself. It will also be very small compared to the typical parasitic capacitances in the wiring. In order to extract the small contribution of the MUT to the capacitance it is necessary to subtract the much larger capacitances of the IDCS, associated electronics and wiring. To this end we can use the method originally proposed in Ref. [24]. This method was used successfully by our research group to measure capacitance variations of a sharp pointer electrode due to a dielectric surface in close proximity [25]. Basically, the method consists of using another interdigitated device, ideally identical to the IDCS as a reference. A driving voltage of fixed frequency f_d is applied to both, the sensor and the reference devices. The output voltages are then subtracted. The idea is that in the absence of a MUT the output signal is ideally zero.

In the original method the subtraction was accomplished by introducing a phase difference of 180° to the voltage applied to the reference device. Here we use a slight variation of the method. We simply feed the output voltages of the sensor and reference device to the non-inverting and inverting inputs of an instrumentation operational amplifier (IOA). This modification makes the system more stable over time. The output voltage from the IOA is analyzed with a lock-in amplifier.

We refer to this condition as the system being balanced. In practice an output voltage of exactly zero is not possible, but one seeks to make the output voltage as small as possible. The advantage of using a balancing scheme is two-fold. On the one hand, we have that when the IDCS and the reference device are as similar as possible the system becomes less sensitive to ambient noise, since these affect both, the sensor and reference equally, and the changes in the output voltages are equal for both devices and cancel out upon subtraction. On the other hand, when a MUT is placed on top of the IDCS the capacitance change and the system becomes unbalanced and a small signal appears, but it does so from a null background, allowing one to amplify the signal by a large factor without saturating the amplifier. In practice, to achieve a nearly null output it is necessary to have a conditioning circuit to make fine adjustments to the reference voltage, since the capacitance of the reference device and the parasitic capacitances associated with it will never be identical to those of the sensor device. Therefore it is necessary to introduce a compensation stage to balance the system and make the output signal as close to zero as possible.

A block diagram of the TCMS proposed here is shown in Fig. 4. It is formed by the IDCS, a compensation stage, a differential stage and a Lock-in amplification stage.

The compensation stage is formed of three sub-stages, Phase Compensation, Amplitude Compensation and Stray Calibration Capacitor. The function of the Phase Compensation sub-stage is to compensate the signal phase variable $V_{ac}(\omega \pm \Phi)$ due to stray capacitances of the conditioning electronics. The Amplitude Compensation sub-stage allows us to compensate the amplitude voltage of the Phase Compensation output as $GV_{ac}(\omega \pm \Phi)$ where G is the amplification factor. The output voltage of this sub-stage is supplied to the Reference Interdigitated Capacitor (RIDC) in order to obtain the same amplitude and phase as the excitation voltage $V_{ac}(\omega)$ applied to the IDCS.

The output signal of the Differential Stage goes into a Lock-in Amplifier (We used a SR850 Stanford Research) to measure and register the temporal differential changes of output voltage.

The internal oscillator of the Lock-in Amplifier generates the excitation voltage $V_{ac} = 1$ V_{rms} at $f_d = 10$ KHz reference frequency which is used to feed the system. The same Lock-in amplifier detects the output differential-signal in a 10 KHz central frequency with a 1.2 Hz bandwidth in order to reduce surrounding noise.

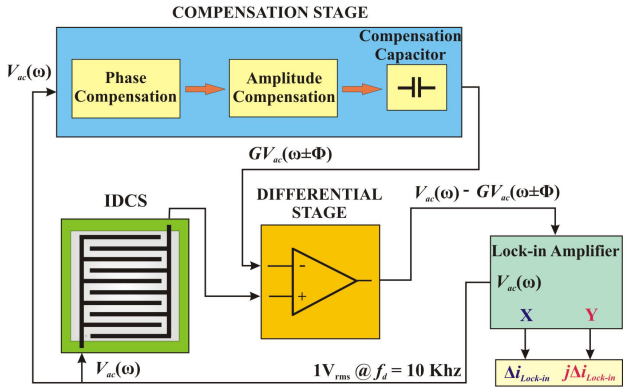

FIGURE 4. Block diagram of the Temporal Capacitive Measurement System (TCMS).

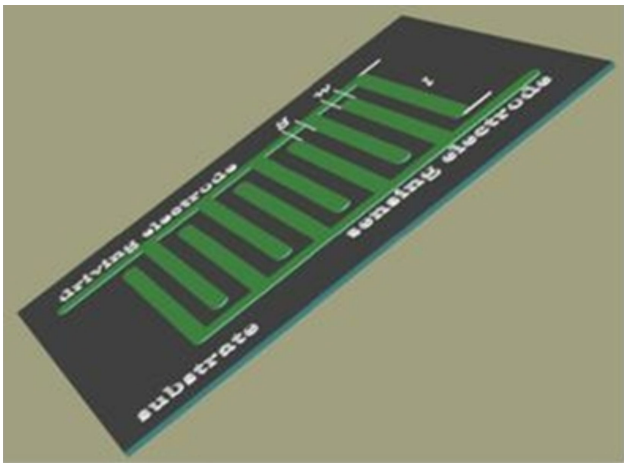

FIGURE 5. Interdigitated Capacitors used in our TCMS as the sensor and reference device.

The capacitance change ΔC when a MUT is present above the IDCS is obtained from the increment of the imaginary part of the current entering the Lock-in amplifier, $\Delta i_{\text{Lock-in}}$. We have [26],

$$\Delta C = \frac{Im[\Delta i_{\text{Lock-in}}]}{\omega V_{ac}}. \tag{5}$$

where $\omega = 2\pi f_d$.

We fabricated a TCMS following the block diagram in Fig. 4. The IDCS used in the proposed TCMS, has ten plane conductive electrodes or fingers parallel each other, five common electrodes form the driving electrode and the rest form the sensing electrode as shown in Fig. 5. The electrodes are placed over a dielectric substrate with sensitive surface of 20×14 mm^2, gap $g = 1$ mm, width $w = g$ and electrode thickness $h_e = 35$ μm. The electrodes were fabricated on a FR-4 Printed Circuit Board (PCB) using conventional techniques. The sensitivity of the IDCS can be increased with the number of fingers and the dimensions of the parameters mentioned before [11].

In order to test and characterize the performance of the constructed TCMS we performed some monitoring experiments. One of our interests in this type of TCMS's is to monitor physico-chemical processes in liquids. Therefore, we chose for the purpose of illustrating the resolution of the TCMS to monitor the evaporation of liquid solvent films. We also attempt to explain the behavior of the temporal evolution of the capacitance signal through qualitative modeling.

4. Experimental evaluation of a TCMS

Interdigitated capacitance sensors have been used for some time to monitor the drying kinetics of coating films [27-31]. The capacitance signal is sensitive to the evaporation of the solvent and the curing stages in the formation of a coating as well as in adhesives and epoxies [32].

Characterization of coatings like polymer thin films is important for capacitive sensors and microelectronics fabrication. Curing process and evaporation solvent of the polymer coating can alter its electric and mechanical properties. So, it is important to measure changes in dielectric constant and thickness of the polymeric thin film especially in the curing process where the temperature is critical for the complete curing of the polymer [33,34].

4.1. Monitoring the evaporation of a thin liquid film

Here we used the IDCS to monitor the evaporation of liquid solvents in order to characterize and evaluate the sensitivity and resolution of the proposed TCMS. We measured the time-evolution of the capacitance during the evaporation of a thin liquid film just above the interdigitated electrodes. To perform the experiments it was necessary to place a cuvette on top of the IDCS to form and hold the liquid film on top of the electrodes. We used a glass cuvette with 100 μm thick walls. Thus, in the experiments the sensor consisted of the interdigitated electrodes with a glass slab on top. The MUT is the liquid dispensed on the glass cuvette forming a thin film on its bottom and the glass slab is the bottom wall of the cuvette as show schematically in Fig. 6.

The experimental procedure was as follows. The TCMS was balanced without a cuvette on its top and obtained an average base line of 30 aF for a 60 min period in our laboratory at ambient temperature and humidity (23°C and 21% H_r average). The balancing was achieved by tuning the phase and amplitude of the reference signal at the input of the reference device. Next we placed a square glass cuvette on top of the sensing device and tuned the reference signal again to recover a minimal output current. We obtained a baseline signal without a noticeable drift and a rms noise around 50 aF/$\sqrt{\text{Hz}}$. The bottom of the cuvette was a 100 μm thick glass slide of about

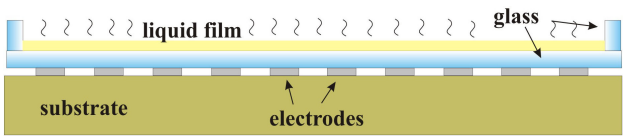

FIGURE 6. Cross section view of the Interdigitated Capacitance Sensor with glass cuvette and solvent sample used in experiments.

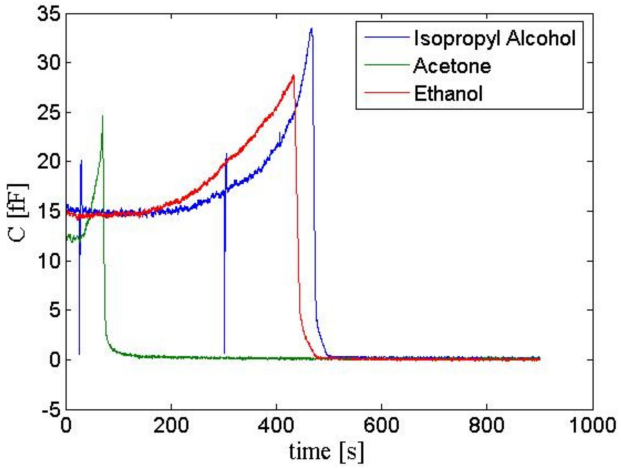

FIGURE 7. Evaporation monitoring curves of Isopropyl Alcohol, Acetone and Ethanol.

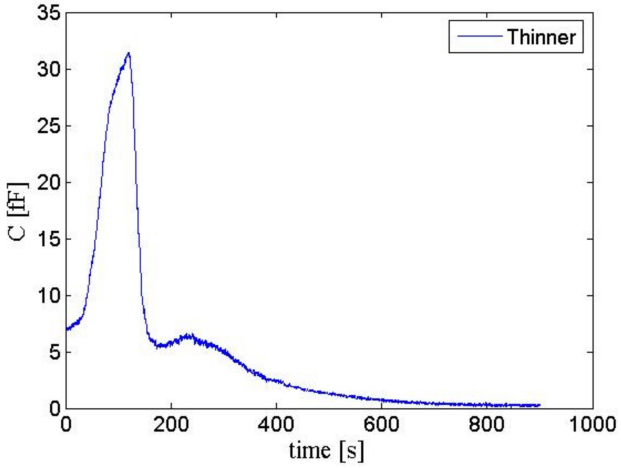

FIGURE 8. Evaporation monitoring curve of Thinner.

330 mm^2 sensitive area. Then a 30 μl volume of solvent sample was deposited in the cuvette forming a liquid film about 100 μm thick.

We monitored the evaporation of isopropyl alcohol, acetone, ethanol and thinner. The first three liquids are pure substances whereas thinner is a mixture of different substances. In Figs. 7 and 8 we show the capacitance change versus time as the liquid films evaporate. In Fig. 7 we show those for the pure liquids and in Fig. 8 that of thinner. In Fig. 7 we can see that as a pure liquid film evaporates the capacitance increases, and it does so at an accelerating rate. At some point, the liquid film evaporates completely and the capacitance drops sharply returning to its base line. In Fig. 8 the same behavior is observed at the beginning but after a sharp drop of the capacitance, the signal does not recover the base line, it starts to increase again and then returns slowly to the base line. This behavior is more complicated probably because the liquid is a mixture of substances and these evaporates at different rates.

Clearly the behavior of the capacitance curves do not correspond simply to a dielectric film reducing its thickness while the rest of the parameters remain constant, since in this case one would see a signal decreasing in time monotonously (see Fig. 3). We monitored the weight reduction in time during the evaporation of the liquid layers presented in Fig. 7 and verified it was constant during the entire process. For completeness of this work, we try to provide a plausible explanation of the behavior of the capacitance signal in Fig. 7.

Nevertheless, the experimental results in Fig. 7 and 8 serve well our purpose. We can estimate from the experimental graphs in the figures that the output signal TCMS has a rms noise around 50 aF/$\sqrt{}$Hz (equivalent to $\sim$ Im [3pA] of the output current). This later value was obtained from the output signal of the Lock-in amplifier used in our TCMS (Standford Research model SR850). This means that in a 1.2 Hz bandwidth the minimum detectable change in capacitance is in the order of 100 aF. Also, we can appreciate in Fig. 7 that the base line remained basically constant for at least 900 seconds. We must point out that this resolution and stability was achieved at ambient conditions without any special care in isolating the TCMS from the environment.

4.2. On the behavior of the capacitance signal

To explain the behavior of the capacitance curves during the evaporation of the solvent films it is necessary to consider the contribution to the capacitance change of the vapor above the liquid. To this end we will derive an approximate formula containing the leading terms for the time derivative the capacitance during the evaporation process using an equivalent circuit analysis. Here we will only consider the signal of the evaporation of pure liquids shown in Fig. 7, since it is simpler. Let us refer to the interdigitated electrodes with glass slab as the sensor. We can consider the capacitance of the sensor as the sum of a large number of elementary capacitances placed in parallel. Each elementary capacitor is formed by a thin strip of space around an electric field line going from one electrode to another. The electric field of many of these elementary capacitors emanating from a given electrode go above the glass slab into the liquid film and air above it and then go back towards another electrode. The capacitance of any given elementary capacitor sensitive to the liquid consists of three capacitances in series,

$$\frac{1}{C} = \frac{1}{C_1} + \frac{1}{C_L} + \frac{1}{C_2}. \tag{6}$$

Where C_1 is the contribution of the electric field lines traversing the glass, C_L is due to their path through the liquid film, C_2 is due to their path through the air above the liquid. Each of the capacitors may be considered as parallel plate capacitor with effective areas and thicknesses. We can write,

$$C_1 = \frac{\varepsilon_1 A}{d_1}, \quad C_L = \frac{\varepsilon_L A}{d_L}, \quad \text{and} \quad C_2 = \frac{\varepsilon_2 A}{d_2}. \tag{7}$$

When the liquid is dispensed on top of the sensor, the dielectric constant ε_2 is that of air. However, when the liquid starts to evaporate the air above the sensor contains vapor molecules and its dielectric constant increases. On the other

hand, as the liquid layer evaporates its thickness decreases and the effective thickness of the liquid layer decreases while the effective thickness of the air capacitor increases. That is, the effective thicknesses involved in C_L and C_2 capacitors are not independent. Assuming the path of the electric field lines do not change considerably upon dispensing the liquid film and during its evaporation we can write,

$$d_L(t) + d_2(t) = d_2^{(0)}, \tag{8}$$

where $d_2^{(0)}$ is equal to the effective thickness of the air capacitor without a liquid layer. When the liquid is dispensed on top of the sensor d_L has its maximum, $d_L(0)$. For simplicity we can assume that the dielectric constant of air is ε_0, and while the liquid layer evaporates it increases due to the incorporation of vapor solvent molecules to

$$\varepsilon_2(t) = \varepsilon_0 + \varepsilon_0 \alpha_m \rho \mathrm{v}(t), \tag{9}$$

where α_m is the molecular polarizability of the solvent molecules and $\rho \mathrm{v}(t)$ is the number density of vapor molecules. Since the number of molecules in the vapor is equal to the number of molecules lost from the liquid, we can write,

$$\rho_L[d_L(0) - d_L(t)] + \rho \mathrm{v}(t) d_2(t) = 0, \tag{10}$$

where ρ_L is the number density of molecules in the liquid phase and can be assumed to be independent of time. The latter equation simply expresses that the molecules leaving the liquid film are incorporated to the vapor. We can use $d_2(t) = d_2^{(0)} - d_L(t)$ in the latter equation. We are assuming that the density of molecules in the liquid remains constant but the density of molecules in the vapor layer and its thickness can both change in time.

Now, to understand the rate of change in capacitance as the liquid evaporates let us take the derivative with respect to time of Eq. (6). Taking the partial derivative of Eq. (6) and using Eq. (7) yields,

$$\frac{\partial}{\partial t}\left(\frac{1}{C}\right) = \frac{\partial}{\partial d_L}\left(\frac{1}{C}\right)\frac{\partial d_L}{\partial t}. \tag{11}$$

Now, the rate of change of the liquid thickness can be assumed constant since the rate of weight reduction in time is constant (as we could verify with an analytical balance) and the area covered by the liquid was constant in time. Thus we can use, $\partial d_L/\partial t \equiv -\beta$, where β is a positive constant.

Evaluating the derivative with respect to d_L of $1/C$ requires using the relation,

$$\frac{\partial \varepsilon_2}{\partial d_L} = \varepsilon_0 \alpha_m \frac{\partial \rho \mathrm{v}}{\partial d_L}, \tag{12}$$

which is obtained from Eq. (9), and

$$\frac{\partial \rho \mathrm{v}(t)}{\partial d_L} \approx \frac{-\rho_L}{d_2^{(0)}}, \tag{13}$$

which is obtained from Eq. (10). Additionally we can assume that $d_2^{(0)} \gg d_L(t)$. Then if we use $\varepsilon_L \gg \varepsilon_2$ and keep only the leading terms we get,

$$\frac{\partial}{\partial d_L}\left(\frac{1}{C}\right) \approx \frac{1}{\varepsilon_2 A}\left(1 - \frac{\varepsilon_0}{\varepsilon_2}\alpha_m \frac{d_2}{d_2^{(0)}}\right). \tag{14}$$

Then, we can approximate $\varepsilon_0/\varepsilon_2 \approx 1$ and $d_2/d_2^{(0)} \approx 1$ in the latter equation. Using this result in Eq. (11) and solving for $\partial C/\partial t$ from the following equality,

$$\frac{\partial}{\partial d_L}\left(\frac{1}{C}\right) = -\frac{1}{c^2}\frac{\partial C}{\partial t}, \tag{15}$$

finally yields,

$$\frac{\partial C}{\partial t} \approx \frac{C^2}{\varepsilon_0 A}(\alpha_m \rho_L - 1)\beta. \tag{16}$$

This equation tells us that the time derivative of the capacitance is positive whenever $\alpha_m \rho_L > 1$ (recall that β is positive). This latter inequality is in general true when the dielectric constant of the liquid is larger than 2, as can be deduced from Clausius-Mossotti equation [35],

$$\rho_L \alpha_m = \frac{3(\varepsilon_L - 1)}{\varepsilon_L + 2}, \tag{17}$$

where ε_L is the dielectric constant of the liquid. Now, it is known that the Clausius-Mossotti relation is accurate for non-polar liquids and no so accurate for polar liquids [36]. But, for polar liquids the molecular polarizability is larger than that predicted by the Clausius-Mossotti relation. Therefore, we conclude that $\rho_L \alpha_m$ is in general larger than one whenever the dielectric constant is larger than 2, and in these cases the rate of change of the capacitance given by Eq. (16) is positive.

Additionally, Eq. (20) tells us that the rate of change of the capacitance increases in time since it is proportional to C^2 and C increases with time. This behavior is maintained until all the liquid evaporates and the vapor layer diffuses away. At this point the capacitance signal should drop to its initial value before the liquid was dispensed over the sensor. That is, the capacitance signal returns to its base line. As already said this is the behavior of the capacitance signal shown in Fig. 7.

In summary, our analysis indicates that the concentration of vapor molecules above the evaporating liquid is responsible for the rather surprising behavior of capacitance signal observed in the experiments.

5. Summary and Conclusions

We studied the sensitivity and resolution of interdigitated capacitance sensors to sense a liquid film on top of it. In sensors with a number of electrodes between 5 and 10 with dimensions in the range of millimeters, the capacitance will vary in the range of tens of femto-Farads due to changes in

layer of thickness in the range of millimeters. To sense small variations of the thickness and dielectric constant of a liquid film and its surroundings, a resolution in the sub-femtoFarad range is required.

We proposed and demonstrated experimentally a differential capacitance measuring system providing a resolution in capacitance variations in the 100 atto-Farad range and a dynamic range in the femto-Farad range. This resolution and dynamic range is sufficient to sense variations in a dielectric layer on top of an interdigiated sensor with ten electrodes of width 1 mm and length 9 mm, separated by a gap of 1 mm. We illustrated the performance of the developed system by monitoring the evaporation of a liquid layer in a glass cuvette on top of the sensor. The results show experimentally that the system provides sufficient resolution and stability to monitor the process under ambient laboratory conditions. However, the behavior of the capacitance signal during the evaporation process was rather unexpected, and thus, we also analyzed these particular experiments with an equivalent circuit approach in order to provide a plausible explanation of the behavior of the signal.

Acknowledgments

The authors want to thank Dirección General de Asuntos del Personal Academico (DGAPA) from Universidad Nacional Autonoma de Mexico for financial support of AGS's postdoctoral work.

1. P. Wang, Quingjung Liu editors, *Engineering in Medicine & Biology*, (2010) Artech House, ISBN-13: 978-1-59693-439-9.
2. Jun Wam Kim, *"Development of Interdigitated Capacitor Sensor for Direct and Wireless Measurements of the Dielectrics Properties of Liquids*", (PhD thesis The University of Texas at Austin, December 2008).
3. V. Mamishev, S. R. Kishore, F. Yang, Y. Du, and M. Zahn, *Proceedings of the IEEE* **92** (2004) 808-845.
4. P. Van Gerwen *et al.*, *Sensors and Actuators B* **49** (1998) 73-80.
5. L. Montelius, J. Tegenfeldt and T. Ling, *J. Vac. Sci. Technol. A* **13** (1995) 1755-1760.
6. P. Jacobs *et al.*, *Impedimetric detection of nucleic acid hybrids* (Proceedings of the Second International Conference on Microreaction Technology, New Orleans, LA, March, 1998) pp. 8-12.
7. N. F. Shepard, D. R. Day, H. L. Lee and S. D. Senturia, *Sensors and Actuators* **2** (1982) 263-274.
8. M. C. Zaretsky, L. Mouayad, and J. R. Melcher, *IEEE Transactions on Electrical Insulation*, **23** (1988).
9. Hagleitner, A. Hierlemann, D. Lange, A. Kummer, N. Kerness, O. Brand and H. Baltes, *Nature* **414** (2001) 293-296.
10. R. Casalini, M. Kilitziraki, D. Wood and M. C. Petty, *Sensors and Actuators B* **56** (1999) 37-44.
11. F. Starzky, *Archives of Materials Science and Engineering*, **34** (2008) 31-34.
12. I. N. Court, *IEEE Trans. Microwave Theory Tech.* no. MTT-17, (1969) 968-986
13. G. D. Alley, *IEEE Trans. Microwave Theory Tech.* MTT-18, (1970) 1028-1033.
14. R. K. Hoffman, *Handbook of Microwave integrated circuits*, (Artech, Norwell, MA, 1987).
15. N. Delmonte, B. E. Watts, G. Chiorboli, P. Cova, and R. Menozzi, *Microelectronics Reliability* **47** (2007) 682-685.
16. V. Mamishev, *Interdigital dielectrometry sensor design and parameter estimation algorithms for non-destructive materials evaluation.* (Department of Electrical Engineering and Computer Science, Massachusetts Institute of Technology, 1999).
17. Kishore Sundara-Rajan, Alexander V. Mamishev, and Markus Zahn, *Fringing Electric and Magnetic Field Sensors Encyclopedia of Sensors*, **X** (2006) 1-12.
18. B.V.N. Nagavarama, Hemant K.S. Yadav, A. Ayaz, L.S. Vasudha, and H.G. Shivakumar, *Different techniques for preparation of polymeric nanoparticles- a review*, Asian Journal of Pharmaceutical and Clinical Research, vol 5, suppl. 3, (2012).
19. G. Brian Prevo and O. D. Velev, *"Controlled, Rapid Deposition of Structured Coatings from Micro- and Nanoparticle Suspensions*, *Langmuir* **20** (2004).
20. Xiaohui Hu and Wuqiang, *Sensor Review*, **301** (2010) 24-39.
21. L. Alfredo Ramajo, D. Enrique Ramajo, M. Marta Reboredo, Diego Hernan Santiago, Miriam Susana Castro, *Materials Research*, **11** (2008) 471-476.
22. A. García-Valenzuela and A. Guadarrama-Santana, *Am. J. Phys*. **78** (2010) 1376-1378.
23. H. A. Majid, N. Razzali, M. S. Sulaiman, and A. K. A'ain, *A capacitive Sensor Interface Circuit Based on Phase Differential Method, World Academy of Science, Engineering and Technology* **55** (2009).
24. D. T. Lee, J. P. Pelz and Bharat Bhushan, *Review of scientific Instruments* **73** (2002) 3525-3533.
25. A. Guadarrama-Santana and A. García Valenzuela, *Review of Scientific Instruments* **80** (2009) 106101.
26. A. Guadarrama-Santana and A. García Valenzuela, *Rev. Mex. Fis.* **55** (2009) 477-485.
27. Liliane Masschelein - Kleiner, *Los Solventes* (2004). ISBN: 956-244-166-0.
28. G. D. Verros and M. A. Malamataris, *Ind. Eng. Chem. Res.* **38** (1999) 3572-3580.
29. Peiming Wang, Andrzej Aderko, *Fluid Phase Equilibria* **186** (2001) 103-122.
30. Niall J. O'reilly and Edmond Magner, *Langmuir*, **21** (2005) 1009-1014. http://lounge.ssradiouk.com/listen.plsonstant

31. L. Goncalves Dias Mendoca, *Interdigitated capacitive sensor to verify the quality of ethanol automotive fuel ABCM Symposium Series in Mechatronics* **3** (2008) 580-585.

32. D. Schlicker, I. Shay, A. Washabaugh, N. Goldfine and B. Givot, *Capacitive sensing dielectometers for noncontact characterization of adhesives and epoxies*, (SPE ANTEC, May 2002).

33. K. S. Patel, P. A. Kohl and S. A. Bidstrup Allen, *Journal of Polymer Science; Part B Polymer Physics* **38** (2000) 1634-1644.

34. Zikang Pan, P. J. Hesketh and G. J. Maclay, *Journal of Vacumm Science & Technology A* **11** (1993) 1396.

35. U. Felderhof, G. W. Ford, E. D. G. Cohen, *Journal of Statistical Physics* **33** (1983).

36. S. Sivasubramanian, A. Widom, Y. N. Srivastava, *Physica A* **345** (2005) 356-366.